Tight-binding study of the electron-phonon interaction in bcc transition metals and alloys

G. Fletcher and J. L. Fry
The University of Texas at Arlington, Arlington, Texas 76019

P. C. Pattnaik
IBM Thomas J. Watson Research Center, Yorktown Heights, New York 10598

D. A. Papaconstantopoulos
Naval Research Laboratory, Washington, D.C. 20375

N. C. Bacalis
Research Center of Crete, Heraklion, Crete, Greece

(Received 6 April 1987; revised manuscript received 16 November 1987)

The tight-binding method has been used to study the electron-phonon interaction in several bcc transition metals and alloys. Slater-Koster fits to self-consistent, scalar-relativistic, augmented-plane-wave band calculations have been employed and scaling relations were used in determining gradients of the tight-binding matrix elements. The two-center integral parameters were adjusted for alloys in a way which explicitly accounts for the change in lattice constant. Results for 3*d* and 4*d* transition-metal elements are in good agreement with rigid-muffin-tin calculations. In addition, the electron-phonon coupling in Mo_xNb_{1-x} is evaluated from densities of states calculated by the coherent-potential approximation. The measured variation of the superconducting transition temperature as a function of x is reproduced well by this calculation.

I. INTRODUCTION

An understanding of the electron-phonon interaction (EPI) in metals has been obtained by the rigid-muffin-tin approximation (RMTA) of Gaspari and Gyorffy[1] and from pseudopotential theory.[2] The RMTA has been used in a systematic study of the superconducting properties of cubic metals,[3] and errors in the Gaspari-Gyorffy approximation for the simple metals were accounted for in a study of the EPI by Zdetsis *et al.*[4] For cubic transition metals and compounds, the Gaspari-Gyorffy approximation appears to work well.[3,5]

Another approach to the calculation of the EPI is the tight-binding approximation (TBA).[6,7] This approach has the advantage of ease of extension to hexagonal systems and alloys. The purpose of this paper is twofold: first, to present an independent check of calculations of the EPI in bcc transition-metal elements using an orthogonal TBA method. Second, to report the results of an application of this method to binary transition-metal alloys using rigid-band or virtual-crystal arguments as well as the coherent-potential approximation (CPA).

Section II of this paper contains a description of the general method used in calculating the matrix element $\langle I^2 \rangle$, the EPI parameter, in the orthogonal TBA. Section III contains a description of the specific application of the TBA to transition metals, along with a discussion of the scaling laws used in calculating gradients of the tight-binding matrix elements. Results for several bcc elements are presented. A description of the application of the TBA to binary alloys is contained in Sec. IV. Conclusions are presented in Sec. V.

II. TIGHT-BINDING APPROXIMATION

The quantity to be calculated is the EPI parameter $\langle I^2 \rangle$,[5,6] defined as

$$\langle I^2 \rangle = \frac{1}{[N(E_F)]^2} \sum_{\mu,\mu'} \int_{\mathrm{FS}} \frac{d\sigma_{\mathbf{k}}}{|\nabla_{\mathbf{k}} E_{\mathbf{k}\mu}|} \int_{\mathrm{FS}} \frac{d\sigma_{\mathbf{k}'}}{|\nabla_{\mathbf{k}'} E_{\mathbf{k}'\mu'}|} \sum_{\alpha} |g^{\alpha}_{\mathbf{k}\mu,\mathbf{k}',\mu'}|^2 . \quad (1)$$

This constitutes a Fermi-surface (FS) average of the electron-phonon matrix element[6]

$$g^{\alpha}_{\mathbf{k}\mu,\mathbf{k}'\mu'} = \sum_{m,n} A^{\dagger}_{\mu m}(\mathbf{k})[\gamma^{\alpha}_{mn}(\mathbf{k}) - \gamma^{\alpha}_{mn}(\mathbf{k}')] A_{n\mu'}(\mathbf{k}') , \quad (2)$$

for scattering between band μ at wave vector $\mathbf{k}$ and band μ' at $\mathbf{k}'$. α refers to x, y, and z components, $A_{\mu m}(\mathbf{k})$ is the mth component of the eigenvector for band μ, and

$$\gamma^{\alpha}_{mn}(\mathbf{k}) = \sum_{i} (\nabla_{\alpha i} \langle \Phi_{0m} | H | \Phi_{in} \rangle) e^{i\mathbf{k}\cdot\mathbf{R}_i} . \quad (3)$$

$N(E_F)$ is the density of states at the Fermi energy. In Eq.

(3), Φ_{0m} is the mth atomiclike basis function at the origin and Φ_{in} is the nth function located at position $\mathbf{R}_i$ in a tight-binding representation of the Hamiltonian, H, for the solid. Using transformation properties of the spherical-harmonic orbital basis, Eqs. (1)–(3) result in the simplified expression[6]

$$\langle I^2\rangle = 2\sum_l \frac{a_l D_l}{d_l} - 2\sum_{m,n,\alpha} C^{\alpha}_{mn} C^{\alpha}_{nm} , \tag{4}$$

where

$$a_l = \frac{48}{N(E_F)} \sum_{\mu} \int_{\mathrm{IFS}} \frac{d\sigma_{\mathbf{k}}}{|\nabla_{\mathbf{k}} E_{\mathbf{k}\mu}|} \sum_m |A_{m\mu}(\mathbf{k})|^2 , \tag{5}$$

$$D_l = \frac{48}{N(E_F)} \sum_{\mu} \int_{\mathrm{IFS}} \frac{d\sigma_{\mathbf{k}}}{|\nabla_{\mathbf{k}} E_{\mathbf{k}\mu}|} \sum_{m,\alpha} \left| \sum_n A_{n\mu}(\mathbf{k}) \gamma^{\alpha}_{nm}(\mathbf{k}) \right|^2 , \tag{6}$$

and

$$C^{\alpha}_{mn} = \frac{1}{N(E_F)} \sum_{\mu} \int_{\mathrm{IFS}} \frac{d\sigma_{\mathbf{k}}}{|\nabla_{\mathbf{k}} E_{\mathbf{k}\mu}|} \sum_{m',i} A_{m\mu}(\hat{\beta}_i \mathbf{k}) A_{m'\mu}(\hat{\beta}_i \mathbf{k}) \gamma^{\alpha}_{m'n}(\hat{\beta}_i \mathbf{k}) . \tag{7}$$

$\hat{\beta}_i$ is the transformation matrix for the ith member of the symmetry group of $\mathbf{k}$. The integrals extend over the portion of the Fermi surface in the irreducible wedge of the first Brillouin zone (IFS). d_l is the dimension of the lth irreducible representation of the cubic group, so that for s, p, and d electrons, there are four subsets corresponding to $l=1,2,3,4$ with $d_l=1,3,3,2$ for the usual ordering: (s), (x,y,z), (xy,yz,zx), and $(x^2-y^2, 3z^2-r^2)$.

The success of the present work depended on the availability of very accurate band structures of the elemental bcc metals in a Slater-Koster representation,[7,8] accurate numerical methods for performing Brillouin-zone integration,[9] and a simple, systematic method for obtaining gradients of the potential matrix elements in the TBA. These will be discussed in Sec. III.

III. APPLICATION TO TRANSITION-METALS

Slater-Koster representations of the band structures of the bcc transition metals have been obtained by fitting self-consistent, scalar-relativistic, augmented-plane-wave (APW) calculations.[8] The orthogonal, two-centered version of the Slater-Koster method was employed in this work and first, second, and third neighbor interactions were retained in the tight-binding Hamiltonian. The typical rms deviation in these calculations was 5 mRy for the first six bands.

The various Fermi-surface integrals were evaluated using the analytic-tetrahedron method, including full variation of matrix elements throughout the zone. Tests of convergence of the integration grid size were made to ensure accurate results.[9]

The scaling laws of Harrison[10] have been used to determine the gradients of the tight-binding Hamiltonian matrix elements in Eq. (2). The advantage of the scaling laws lies in the fact that it is not necessary to have band structures at several lattice constants to calculate electron-phonon matrix elements. The scaling laws may be more reliable in estimating the gradients than band calculations at two lattice constants differing by a small amount because of the numerical sensitivity of the latter. In this scaling method, the ss, sp, and pp bond parameters were varied as R^{-2}, the sd and pd as $R^{-7/2}$, and the dd as R^{-5}, where R is the bond length.[10]

No other approximation was made in the calculation. Group theory was used to avoid calculation of quantities which are zero, or equal to a previously computed quantity. In this way the calculations were made feasible for a number of elements. Most of the computer time was spent evaluating the C integrals, given by Eq. (7), which contribute only a few percent of the total in Eq. (4). Details of the procedure are given elsewhere.[7]

Results of the present calculation are shown in Fig. 1 for $3d$ and $4d$ transition metals, compared with the

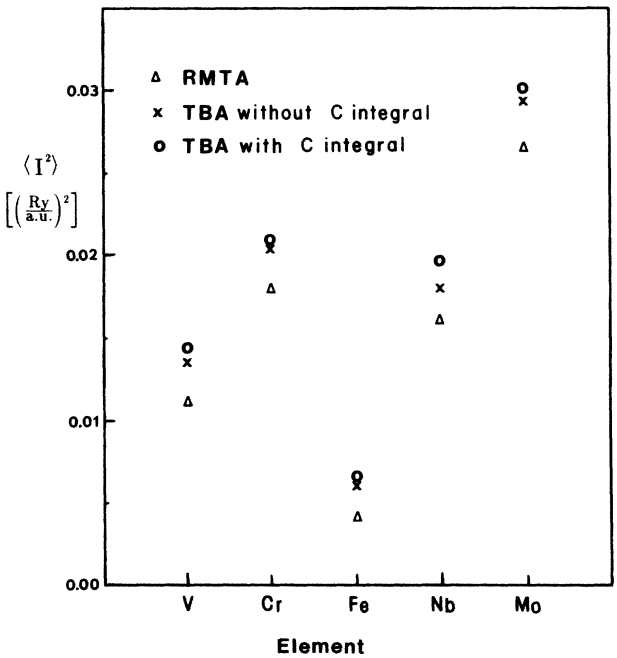

FIG. 1. Electron-phonon interaction parameter $\langle I^2\rangle$ for several transition-metal elements. Plotted are results from Ref. 4 (Δ), present results without the contribution from Eq. (7) (×), and present results with Eq. (7) included (○). All values of $\langle I^2\rangle$ are in (Ry/a.u.)^2.

Gaspari-Gyorffy results of Ref. 3. Agreement is quite satisfactory, as can be seen in the figure, and this supports the general validity of both the TBA and the Gaspari-Gyorffy formulations of the EPI for these elements. This is because although both methods start with the same first principles band structures, the approximations made may be quite different. For obvious reasons both methods fail for simple metals unless corrected. The Gaspari-Gyorffy approximation underestimates and the TBA overestimates $\langle I^2 \rangle$ in simple metals unless corrections are made.[4]

A different set of scaling laws for the two-center integral parameters was suggested by Andersen.[11] In this scheme, *ss* bond parameters vary as R^{-1}, *pp* and *sd* as R^{-3}, *dd* as R^{-5}, and *pd* as R^{-4}. Table I contains a comparison of $\langle I^2 \rangle$ calculated with Harrison scaling and with Andersen scaling. Results with and without the *C*-integral contribution are presented. The difference between the two scaling methods can be seen to be small.

IV. TRANSITION-METAL ALLOYS

In this section the application of the tight-binding approach to the electron-phonon interaction for transition-metal binary alloys is described. First, a description of two methods previously used is given, namely, the rigid-band approximation and the virtual-crystal approximation (VCA). Then an improved method that combines the VCA and the scaling laws is described. Finally we present an evaluation of the EPI using the density of states at the Fermi energy resulting from calculations with the CPA.

A. Rigid-band and virtual-crystal approximations

In the rigid-band approximation to the tight-binding method, it is assumed that the bond parameters will not change significantly as a result of alloying and that the effects of alloying can be accounted for by changing the Fermi energy to accommodate the change in the number of conduction electrons.

One weakness in this approximation is that the energy bands are therefore the densities of states of the two components are not identical. In addition, the energy bands for the resulting alloy will not necessarily be the same as those of the constituent elements.

An even stronger criticism, however, is that the change in the lattice constant upon alloying is not included. Since a change in lattice constant, due to pressure effects, for example, can significantly change the Fermi surface, it is to be expected that a quantity such as $\langle I^2 \rangle$, which has a strong Fermi-surface dependence, will change with the lattice constant.

Table II contains the results of a calculation[12] of $\langle I^2 \rangle$ for the binary alloy A_xB_{1-x} using the rigid-band approximation. The table contains the two extreme cases: that of increasing the number of electrons by one in the element with fewer valence electrons and that of decreasing the number of electrons by one in the element with more valence electrons. Thus, for example, if the rigid-band approximation was accurate, the results of $\langle I^2 \rangle$ for vanadium plus one electron would be the same as $\langle I^2 \rangle$ for chromium, and so on. As can be seen from Table III, the results for Cr_xV_{1-x} and Mo_xNb_{1-x} are not encouraging.

A method which attempts to account for the different band structures of the elements is the virtual-crystal approximation. In this approximation, the bond parameters are taken to be the weighted sum of those of the constituent elements. Thus, for A_xB_{1-x}, the *i*th bond parameter is given by

$$V_i = xV_{iA} + (1-x)V_{iB} \ . \tag{8}$$

However, this approximation does not address the problem of the change in lattice constant upon alloying.

B. Improved approximation

The improved method discussed here combines the VCA given in Eq. (8) with a scaling approximation. The bond parameters for A_xB_{1-x} are written as $V_i = xU_i^A + (1-x)U_i^B$, where the U_i's are the scaled bond parameters. The basis of the Harrison scaling method, which was discussed briefly in Sec. III, is that the quantity $R^{n_i}V_i$ is taken to be invariant under changes in the lattice parameter. Therefore, $R_0^{n_i}V_i^0 = R^{n_i}V_i$, where R_0 is the equilibrium bond length, R is the new bond length, V_0^i is the equilibrium bond parameter, V_i is the new bond parameter, and n_i is chosen according to the kind of bond parameter involved. (See Sec. III.) Thus, in determining the bond parameters for the binary alloys, the variation due to the change in lattice constant is included by defining

$$U_i^A = \left[\frac{R_0^A}{R^A} \right]^{n_i} V_{iA}^0 \ ,$$

where R^A is the new bond length. Then, the bond parameters used in the calculation of $\langle I^2 \rangle$ for A_xB_{1-x} are

TABLE I. A comparison of the results of the present calculations using the Harrison scaling method and the Andersen scaling method. All values are in units of (Ry/a.u.)^2.

Scaling method	$\langle I^2 \rangle$ without *C* integral Cr	Mo	$\langle I^2 \rangle$ with *C* integral Cr	Mo
Harrison	0.0209	0.0298	0.0212	0.0306
Andersen	0.0210	0.0300	0.0217	0.0314

TABLE II. Results of the rigid-band approximation calculation of the electron-phonon interaction parameter from Ref. 12. All values are in units of (Ry/a.u.)^2.

Element	(z)	$\langle I^2 \rangle(z)$	$\langle I^2 \rangle(z+1)$	$\langle I^2 \rangle(z-1)$
V	5	0.0137	0.0173	
Cr	6	0.0209		0.0172
Nb	5	0.0183	0.0272	
Mo	6	0.0298		0.0211

TABLE III. Density of states per spin at the Fermi energy for Mo_xNb_{1-x}. x is the concentration and the units are (states/Ry spin).

x	Rigid band	Scaling	CPA
0.0	9.53	9.53	
0.1	8.41	8.42	7.83
0.3	7.05	7.23	6.69
0.5	5.04	3.67	5.17
0.7	3.00	3.18	3.79
0.9	3.00	3.38	4.46
1.0	3.33	3.80	

given by

$$V_i = x\left[\frac{R_0^A}{R^A}\right]^{n_i} V_{iA}^0 + (1-x)\left[\frac{R_0^B}{R^B}\right]^{n_i} V_{iB}^0 \ . \tag{9}$$

The results of the application of this method are shown in Figs. 2 and 3. Figure 2 shows $\langle I^2\rangle$ versus concentration x for Mo_xNb_{1-x} for known lattice parameters. Included in the figure are the rigid-band approximation results of Ref. 6. The overall trend is the same, with the present results systematically higher. Also included are the results of a KKR-CPA calculation.[13] Agreement is good at the Mo end but the present results are higher at the Nb end of the concentration plot. The dip in $\langle I^2\rangle$ for $0.3 \le x \le 0.5$ appears to be a Fermi-surface effect, since it also was seen in a rigid-band calculation.[6] Figure 3 shows a similar plot for Cr_xV_{1-x}. The overall shape is approximately the same as Mo_xNb_{1-x}, with a larger jump at about $x = 0.6$.

C. Electron-phonon coupling using the CPA

The results presented in Secs. IV A and IV B were obtained from a direct evaluation of the matrix element

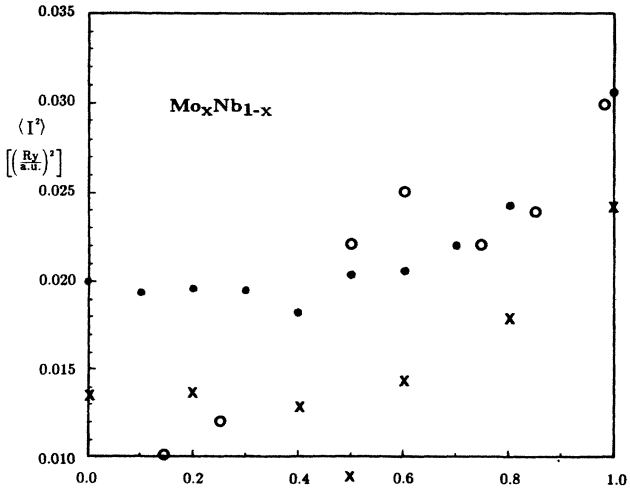

FIG. 2. Electron-phonon interaction parameter $\langle I^2\rangle$ for the binary alloy Mo_xNb_{1-x} for $0 \le x \le 1$. Results from the present calculation are plotted (●), along with results from Ref. 6 (×) and Ref. 13 (○). All values of $\langle I^2\rangle$ are in (Ry/a.u.)^2.

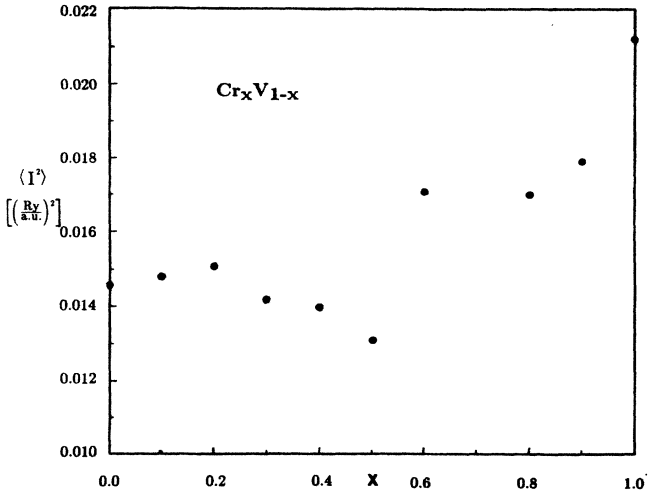

FIG. 3. Results of the present calculation of the electron-phonon interaction-parameter $\langle I^2\rangle$ for the binary alloy Cr_xV_{1-x} for $0 \le x \le 1$. All values of $\langle I^2\rangle$ are in (Ry/a.u.)^2.

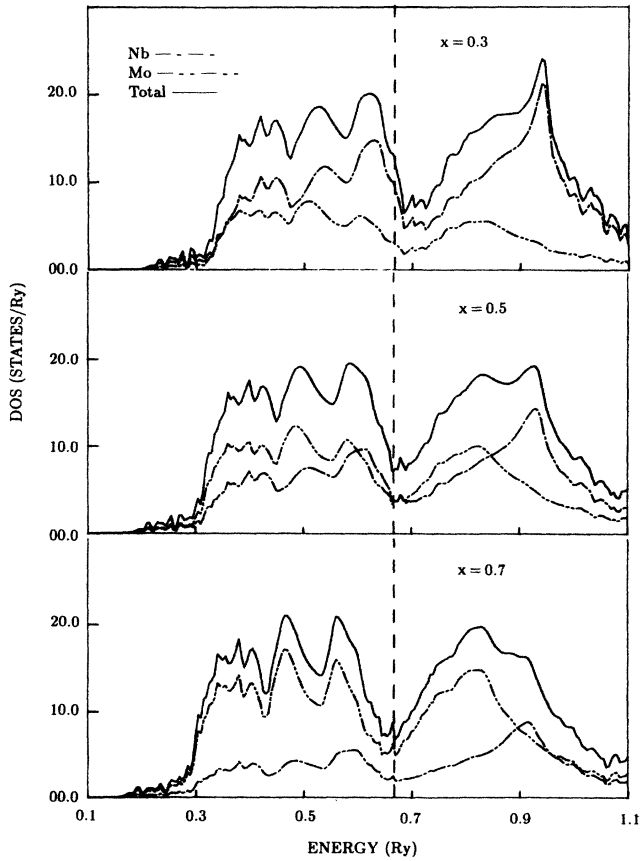

FIG. 4. Plots of densities of states for both spins as a function of energy for different concentrations x in Mo_xNb_{1-x}. The total density of states is plotted as (—), the Nb contribution is plotted as (— - — -), and the Mo contribution as (— ·· — ··). Units are in states/Ry.

TABLE IV. Densities of states per spin at the Fermi energy decomposed into angular momentum components (s,p,d) for each element in Mo_xNb_{1-x}. x is the concentration and the units are (states/Ry spin).

		Mo				Nb			
x	$N(E_F)$	s	p	t_{2g}	e_g	s	p	t_{2g}	e_g
0	9.93	0	0	0	0	0.40	1.04	6.52	1.97
0.10	7.83	0.021	0.161	0.260	0.091	0.200	1.422	4.521	1.154
0.30	6.69	0.079	0.412	0.793	0.312	0.191	0.963	3.164	0.782
0.50	5.17	0.126	0.653	1.080	0.454	0.131	0.650	1.570	0.433
0.70	3.79	0.083	0.541	1.598	0.485	0.037	0.234	0.660	0.150
0.90	4.46	0.083	0.625	2.546	0.866	0.009	0.070	0.207	0.056
1.00	4.02	0.09	0.38	2.45	1.11	0	0	0	0

$\langle I^2 \rangle$ within VCA-like approximations for the band structure of the alloy. It is well known that such approaches often fail to describe accurately the details of the density of states (DOS) in alloys. The method that is best suited for the evaluation of the DOS of an alloy is the CPA. Thus, calculations of the DOS for the Mo_xNb_{1-x} system have been performed using the TB-CPA method. The results of these calculations are shown in Fig. 4 where plots of the DOS for Mo concentrations $x=0.3,0.5$ *and* 0.7 are displayed. It is clear that the gross features of the DOS retain rigid-band characteristics for this system and therefore this offers a justification for the approach used in the previous sections. A more detailed comparison of the CPA results with the other calculations is given in Table III, where $N(E_F)$ as a function of x are listed. It should be noted that in a quantitative sense there are substantial differences between the CPA and the other results. A more complete list of the CPA results with a breakdown of $N(E_F)$ into alloy and angular momentum components is given in Table IV. It would be desirable to calculate rigorously the quantity $\langle I^2 \rangle$ from the results of Table IV but such a formalism is not known in TB-CPA.

In order to gain an understanding of the physical picture emerging from these calculations, the electron-phonon coupling λ and the superconducting transition temperature T_c were calculated. The McMillan-Dynes[14] equation

$$T_c = \frac{\langle \omega \rangle}{1.2} \exp\left[\frac{1.04(1+\lambda)}{\lambda - \mu^*(1+0.062\lambda)} \right] , \tag{10}$$

was used, where

$$\lambda = \frac{N(E_F)\langle I^2 \rangle}{M\langle \omega^2 \rangle} . \tag{11}$$

First, Eq. (10) is inverted to find the value of λ that corresponds to the experimental value of T_c at $x=0$ and $x=1$. $\langle \omega \rangle$ is set equal to $\Theta_D/\sqrt{2}$ and μ^* is chosen to be 0.13. Since the Debye temperature Θ_D as given by McMillan[15] increases monotonically with x and the results of Fig. 2 also show an increase of $\langle I^2 \rangle$ with x, the quantity $\langle I^2 \rangle / M\langle \omega^2 \rangle$ is slowly varying and is taken to be constant. This means that Eq. (11) becomes

$$\lambda_i = \text{const} \times N_i(E_F) , \tag{12}$$

where the index i indicates the alloy component. Equation (12) was used with the CPA results for $N_i(E_F)$ and T_c was calculated from Eq. (10). The results are shown in Table V, which indicates that the rapid decrease of values of T_c is reproduced by this calculation.

V. CONCLUSIONS

A systematic study of the electron-phonon interaction has been presented within the tight-binding approximation for body-centered-cubic transition metals. A comparison was made with a study of the EPI in which the RMTA theory of Gaspari and Gyorffy was employed. It is concluded that the two approaches are equivalent for the 3*d* and 4*d* bcc transition metals, giving results which are in agreement to within a few percent. Some of the differences may be due to the fact that the Gaspari-Gyorffy results are based on nonrelativistic band-structure calculations whereas the Slater-Koster parameters used here were obtained from scalar-relativistic band calculations for the heavier elements.

The tight-binding method was applied to binary alloys

TABLE V. Electron-phonon coupling constant λ and critical temperature T_c for Mo_xNb_{1-x}. $\langle \omega \rangle$ is taken to be $\Theta_D/\sqrt{2}$ (see text). $\langle \omega \rangle$ and T_c are in degrees kelvin and x is the concentration.

x	λ_{Nb}	λ_{Mo}	λ_{tot}	$\langle \omega \rangle$	T_c^{theor}	T_c^{expt}
0	0.88	0.00	0.88	196	9.2	9.2
0.1	0.65	0.04	0.69	208	5.3	6.3
0.3	0.45	0.13	0.58	235	3.3	2.4
0.5	0.25	0.19	0.44	261	0.9	0.2
0.7	0.10	0.22	0.32	286	0.06	0.02
0.9	0.03	0.33	0.36	312	0.23	0.3
1.0	0.00	0.41	0.41	325	0.9	0.9

using an approximation which allows for the change in lattice parameter due to alloying. This method is no more difficult to implement than the rigid-band approximation or the VCA. However, it has a firm theoretical foundation in the scaling method of Harrison.

CPA calculations were also performed for the Mo_xNb_{1-x} alloys which are consistent with the results of the above approaches and provide an evaluation of the electron-phonon coupling and the transition temperature in agreement with experiment.

ACKNOWLEDGMENTS

This work was supported in part by the Robert A. Welch Foundation, the United States Air Force Office of Scientific Research, and the Office of Naval Research.

[1]G. D. Gaspari and B. L. Gyorffy, Phys. Rev. Lett. **29**, 801 (1972).

[2]G. Grimvall, Phys. Scr. **14**, 63 (1976).

[3]D. A. Papaconstantopoulos *et al.*, Phys. Rev. B **15**, 4221 (1977).

[4]A. D. Zdetsis, E. N. Economou, and D. A. Papaconstantopoulos, Phys. Rev. B **24**, 3115 (1981).

[5]B. M. Klein, L. L. Boyer, and D. A. Papaconstantopoulos, Phys. Rev. Lett. **42**, 530 (1979).

[6]C. M. Varma, E. I. Blount, P. Vashishta, and W. Weber, Phys. Rev. B **19**, 6130 (1979).

[7]P. C. Pattnaik, M. Schabes, and J. L. Fry (unpublished).

[8]D. A. Papaconstantopoulos, *Handbook of the Band Structures of Elemental Solids* (Plenum, New York, 1986).

[9]See P. C. Pattanik and J. L. Fry, Solid State Commun. **50**, 601 (1984), and references therein.

[10]W. A. Harrison, *Electronic Structure and the Properties of Solids* (Freeman, San Francisco, 1980).

[11]A. R. Mackintosh and O. K. Andersen, in *Electrons at the Fermi Surface,* edited by M. Springford (Cambridge University Press, Cambridge, 1980), p. 173.

[12]P. C. Pattnaik, G. Fletcher, J. L. Fry, and D. A. Papaconstantopoulos, Bull. Am. Phys. Soc. **30**, 523 (1985).

[13]E. S. Guiliano, R. Ruggeri, E. Donato, and A. Stancanelli, Nuovo Cimento **66**, 118 (1981).

[14]R. C. Dynes, Solid State Commun. **10**, 615 (1972).

[15]W. L. McMillan, Phys. Rev. **167**, 331 (1968).